

# Vibration Suppression for a Beam-Cart System using Adaptive Fuzzy Controller

J. Lin and W.-S. Chao

**Abstract**—Motion and control of a Bernoulli-Euler beam fixed on a moving cart will be analysis in this study. The moving cart is mounted on the ball-screw mechanism system. Dynamic formulation for control purposes is first investigated for such beam-cart system in this research. The controller has two separate feedback loops for positioning and damping, and the vibration suppression controller is independent of linear motion stage positioning control. An experimental apparatus was constructed, constituted of a flexible cantilever aluminum beam type structure with piezoelectric patches symmetrically bonded on both sides to provide structural bending. Strip-bender type piezoelectric patches were attached to the surface of the beam to serve as actuators and sensor, respectively. Experimental validation of for such structure demonstrates the effectiveness of the proposed controller. The results of this study can be feasible to various mechanical systems, such as high tower cranes, ladder cars or overhead cranes.

## I. INTRODUCTION

Many researchers [1-6] have studied dynamic responses of a flexible beam subjected to a moving cart. There has been a lot of research works on the vibration analysis of flexible structures or flexible beams subject to various boundary and load conditions. They arise, for example, in a railroad tracks and bridges traversed by high-speed trains, elevated roadways that support moving vehicles, overhead cranes, high-speed precision machining and computer disk drives used for storage. In each of these systems, estimates of the moving loads and the accurate calculation of the response and stresses of the structures are crucial for a reliable design, the prediction of lifetimes and the implementation of control strategies [7-8].

One kind of such beam-mass systems considered in a vast number of previous studies is a uniform cantilever beam that carries a concentrated mass or body at one end and the other end is fixed or restrained to a large inertial frame or the ground. For example, when the reclaims in automatic warehouses, high tower cranes, ladder cars or overhead

cranes carry heavy loads, the vibrational motion due to the flexibility of the main beam is unavoidable [3-6].

The equations of motion of the beam-mass-cart system are analyzed through unconstrained modal analysis, and a unified characteristic equation for calculating the natural frequencies of the system is established in [3-4]. Moreover, the vibrational motion of an elastic beam fixed on a moving cart and carrying a moving mass is investigated in [5]. However, the above papers are concentrated on the dynamic analysis; no control methodology was presented for such researches. Similarly, reference [6] proposes a modified pulse sequence method with robust internal-loop compensator (RIC) to suppress single-mode residual vibration and to get accurate positioning of the beam-mass-cart system. However, it is only possible to suppress initial vibration, no further vibration reduction discussion during the reciprocal motion.

When used in flexible structures, the piezoelectric materials are bonded to the body of the structure using strong adhesive material. A distinct characteristic of piezoelectric actuators or sensors is that they are spatially distributed over the surface that is being sensed and/or controlled. This property makes them different from the discrete actuators and sensors, which are often used in the control of flexible structures [9-14]. However, all the papers considered above are limited to the vibration control of a laminated beam, and none have presented control methodology for the elastic beam fixed on a moving cart.

In fact, the vibration phenomenon of an elastic beam is strongly affected by the moving cart, especially for reciprocal motion of the cart. Therefore, the motion and control of a Bernoulli-Euler beam fixed on a moving cart will be analysis in this study.

## II. DYNAMIC SYSTEM MODELING

Figure 1 shows the cart-beam system considered in this study. The elastic beam is assumed to follow the Bernoulli-Euler beam model and to be clamped tightly on the moving cart. The base cart moves on the horizontal plane by the applied force  $f(t)$ . The equation of motion and the boundary conditions of the cart-beam system in Fig. 1 are derived by Hamilton's principle as follows [15]

$$m\ddot{x} + \int_0^l [\gamma(\ddot{x} + \ddot{w})] dy = f(t), \quad (1)$$

$$EIw^{(4)} + \gamma(\ddot{x} + \ddot{w}) = 0, \quad (2)$$

$$w(0, t) = w'(0, t) = EIw''(l, t) = EIw'''(l, t) = 0, \quad (3)$$

Manuscript received September 11, 2007. This work was supported in part by the National Science Council of the Republic of China, Taiwan under Grant NSC 95-2221-E-231-010.

J. Lin is with the Department of Mechanical Engineering, Ching Yun University, 229, Chien-Hsin Rd., Jung-Li, Taiwan 320, ROC. (e-mail: jlin@cyu.edu.tw).

W.-S. Chao is with the Department of Mechanical Engineering, Ching Yun University, 229, Chien-Hsin Rd., Jung-Li, Taiwan 320, ROC

where  $m$  is the mass of the cart,  $l$  is the length of the elastic beam,  $\gamma$  is the mass per unit length of the elastic beam,  $EI$  is the flexural rigidity of the unloaded beam,  $x$  is the position of the cart,  $\dot{w} = \partial w(y,t)/\partial t$  and  $w'' = \partial^2 w(y,t)/\partial y^2$ , where  $w(y,t)$  is the deflection of the beam at  $y$ .

Then, assuming a Bernoulli-Euler beam model, the deflection of elastic beam  $w(y,t)$  can be expressed as a summation of the infinite series terms

$$w(y,t) = \sum_{i=1}^n q_i(t)\phi_i(y) \quad (4)$$

where  $q_i(t)$  are generalized modal coordinates and  $\phi_i(y)$  are mode-shape functions that are dependent upon the boundary-value problem. Furthermore,  $n$  is the number of retained modes.

Moreover, natural frequencies of the cart-beam system in Fig. 1 are represented as

$$\omega_i^2 = \frac{EI k_i^4}{\rho_0} \quad (5)$$

where  $k_i$  are the roots of the frequency equation changed along the weight ratios of the cart-beam system and as follows [4]:

$$1 + \cos \xi_i \cosh \xi_i + \frac{r_2}{\xi_i} (\sin \xi_i \cosh \xi_i + \cos \xi_i \sinh \xi_i) = 0, \quad (6)$$

where  $r_2 = \frac{m_b}{m}$ ,  $m_b = \gamma l$ ,  $\xi_i = k_i l$ .

The mode shape function can be obtained as in the following

$$\begin{aligned} \phi_i(y) &= \cosh k_i y - \cos k_i y - \alpha_i (\sinh k_i y - \sin k_i y) \\ \alpha_i &= \frac{\cosh \xi_i + \cos \xi_i}{\sinh \xi_i + \sin \xi_i} \end{aligned} \quad (7)$$

where  $\xi_1 = 1.875104$ ,  $\xi_2 = 4.694091$ ,  $\xi_3 = 7.854757$ ,  $\alpha_1 = 0.734096$ ,  $\alpha_2 = 1.018446$ ,  $\alpha_3 = 0.999225$ ,  $\xi_i = k_i l$  [16].

Furthermore, the kinetic energy,  $K(t)$ , and the potential energy,  $P(t)$ , of the cart and the flexible beam are represented as

$$K(t) = K_r(t) + \int_0^l K_e(y,t) dy \quad (8)$$

$$P(t) = P_r(t) + \int_0^l P_e(y,t) dy$$

where  $K_r(t)$  and  $P_r(t)$  are the kinetic and potential energy functions due to the motion of the cart, and  $K_e(y,t)$  and  $P_e(y,t)$  are the kinetic and the potential energy density functions due to the flexibility of the beam, respectively. Moreover, Equation (8) can be also represented as

$$\begin{aligned} K_r &= \frac{1}{2} m \dot{x}^2 \\ K_e &= \frac{1}{2} \gamma (\dot{x} + \dot{w})^2 = \frac{1}{2} \gamma \left( \dot{x} + \sum_{i=1}^n \phi_i(y) \dot{q}_i(t) \right)^2 \end{aligned} \quad (9)$$

$$P_r = 0$$

$$P_e = \frac{1}{2} EI (w'')^2 = \frac{1}{2} EI \left( \sum_{i=1}^n \phi_i''(y) q_i(t) \right)^2$$

In such case, the cart position  $x$  is not measurable and the ball-screw rotation angle  $\theta$  is measured from the optical encoder, which is attached on the servomotors. Therefore, equation (9) can be rewrite  $x$  as the terms of the rotation angle  $\theta$  ( $x = l_p \theta$ ,  $l_p$  is the lead pitch of the ball-screw) as in the following:

$$\begin{aligned} K_r &= \frac{1}{2} m (l_p \dot{\theta})^2 = \frac{1}{2} m l_p^2 \dot{\theta}^2 \\ K_e &= \frac{1}{2} \gamma (l_p \dot{\theta} + \dot{w})^2 = \frac{1}{2} \gamma \left( l_p \dot{\theta} + \sum_{i=1}^n \phi_i(y) \dot{q}_i(t) \right)^2 \end{aligned} \quad (10)$$

$$P_r = 0$$

$$P_e = \frac{1}{2} EI (w'')^2 = \frac{1}{2} EI \left( \sum_{i=1}^n \phi_i''(y) q_i(t) \right)^2$$

The equations of motion are derived using Lagrangian formulation,

$$\frac{d}{dt} \frac{\partial L}{\partial \dot{X}} - \frac{\partial L}{\partial X} = \tau, \quad (11)$$

with  $X = [\theta \quad q_1 \quad q_2 \quad \dots \quad q_n]^T$ . Hence, the Lagrangian  $L$  can be defined as

$$L = \frac{1}{2} m l_p^2 \dot{\theta}^2 + \frac{1}{2} \gamma \int_0^l \left( l_p \dot{\theta} + \sum_{i=1}^n \phi_i(y) \dot{q}_i(t) \right)^2 dy - \frac{1}{2} EI \int_0^l \left( \sum_{i=1}^n \phi_i''(y) q_i(t) \right)^2 dy \quad (12)$$

The equations of motion for the cart-beam system are

$$M \ddot{X} + D \dot{X} + KX + F_d = B \tau, \quad (13)$$

where  $M$  is the inertia matrix,  $D$  is damping matrix,  $K$  stiffness matrix,  $F_d$  is the equivalent friction torque caused by the motor brushes, support bearing, and nut interfaces; and  $\tau = [u_1 \quad u_2]^T$ . Moreover,  $u_1$  is the motor torque generated by a current-controlled servo-amplifier driven by voltage command from the DSP, and  $u_2$  is the control voltage from the piezo-actuator.

$$M = \begin{bmatrix} (m + \gamma l) l_p^2 & \gamma l_p \int_0^l \phi_1(y) dy & \dots & \gamma l_p \int_0^l \phi_n(y) dy \\ \gamma l_p \int_0^l \phi_1(y) dy & \gamma \int_0^l \phi_1^2(y) dy & \dots & \gamma \int_0^l \phi_1 \phi_n(y) dy \\ \vdots & \vdots & \ddots & \vdots \\ \gamma l_p \int_0^l \phi_n(y) dy & \gamma \int_0^l \phi_n \phi_1(y) dy & \dots & \gamma \int_0^l \phi_n^2(y) dy \end{bmatrix},$$

$$K = EI \begin{bmatrix} 0 & 0 & \dots & 0 \\ 0 & \int_0^l \phi_1'' \phi_1''(y) dy & \dots & \int_0^l \phi_1'' \phi_n''(y) dy \\ \vdots & \vdots & \ddots & \vdots \\ 0 & \int_0^l \phi_n'' \phi_1''(y) dy & \dots & \int_0^l \phi_n'' \phi_n''(y) dy \end{bmatrix}$$

$$B = \begin{bmatrix} 1 & 0 & \cdots & 0 \\ 0 & \phi'(l_0) & \cdots & \phi'_n(l_0) \end{bmatrix}^T$$

where  $l_0$  is the location of the piezoactuator.

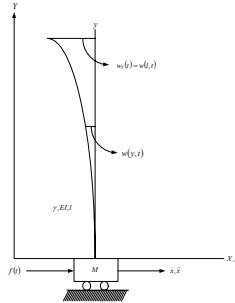


Fig. 1 Conceptual model of the cart-beam system

### III. SYSTEM CONFIGURATION

The experimental system, in Fig. 2 consists of the following components. A Panasonic AC servomotor with encoder is attached to the ball-screw through a noninfluencing helical coupling. In addition, the ball-screw has a low-friction ball-nut around it, which, in turn, is connected to the translating stage. The ball-nut assembly is spring loaded against the ball-screw in an attempt to eliminate backlash in the system. The system is mounted on granite table for vibration isolation and located in a temperature-controlled room [17]. Figure 3 indicates the schematic diagram of the control experiment. The complete system is installed in the Sensor and Control Laboratory at the Department of Mechanical Engineering at Ching Yun University, Fig. 4.

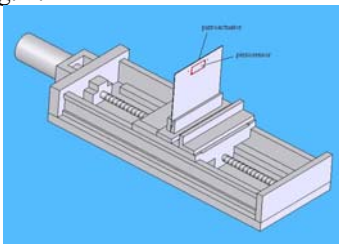


Fig. 2 Schematic view of the system configuration

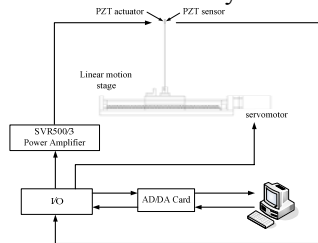


Fig. 3 Schematic diagram of the control experiment

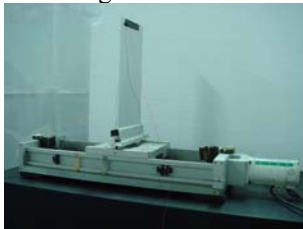


Fig. 4 Experimental apparatus

## IV. CONTROLLER DESIGN

### 4.1 Fuzzy Tracking Controller (FTC)

In this investigation, we consider the neural fuzzy control systems that can be built from a set of input-output training data pairs through hybrid structure-parameter learning. An adaptive network-based fuzzy inference system (ANFIS) has been used to optimize the fuzzy IF-THEN rules and the membership functions to derive a more efficient fuzzy control. The algorithm that uses the Takagi-Sugeno-Kang (TSK) inference system then optimizes the controller. By employing a hybrid learning procedure, the proposed architecture can refine fuzzy if-then rules obtained from human experts to describe the input-output behavior of a complex system [18].

Joint angle tracking error ( $e = \theta_d - \theta$ ) of the moving cart and its rate variable ( $\dot{e}$ ) are two typical variables in fuzzy control system. This investigation uses the ANFIS to optimize fuzzy IF-THEN rules and membership functions for driving a more efficient fuzzy control. Usually we choose  $\mu_{A_i}(x_i)$  to be bell-shaped with maximum equal to 1 and minimum equal to 0, such as

$$\mu_{A_i}(x_i : a_i^j, b_i^j, c_i^j) = 1 / \left[ 1 + \left( \frac{x_i - c_i^j}{a_i^j} \right)^2 \right]^{b_i^j}, \quad (14)$$

where  $\{a_i^j, b_i^j, c_i^j\}$  is the parameter set to be tuned. Moreover, in this research, linguistic variables corresponding to *large negative* (LN), *small negative* (SN), *zero* (ZE), *small positive* (SP), and *large positive* (LP) are used to represent the domain knowledge.

Let us now derive the parameter learning for such system. The derivation procedure is similar to the corresponding author previous work [18]. Assume that  $y^d$  is the desired output for input vector  $\mathbf{x} = [x_1 \ x_2]^T = [e \ \dot{e}]^T$ . The objective error function to be minimized is defined by

$$E = \frac{1}{2} (y - y^d)^2$$

$$= \frac{1}{2} \left[ \frac{\sum_{j=1}^5 \mu_j(\mathbf{x}) w_j}{\sum_{j=1}^5 \mu_j(\mathbf{x})} - y^d \right]^2 = \frac{1}{2} \left[ \frac{\sum_{j=1}^5 \left( \prod_{i=1}^2 \mu_{A_i}(x_i) \right) w_j}{\sum_{j=1}^5 \left( \prod_{i=1}^2 \mu_{A_i}(x_i) \right)} - y^d \right]^2 \quad (15)$$

where  $w_j$  is a crisp number of the consequent part.

Since the shape of the bell-shaped membership function  $\mu_{A_i}(x_i)$  is defined by the parameter set  $\{a_i^j, b_i^j, c_i^j\}$ , the objective function  $E$  consists of the tuning parameters  $a_i^j$ ,  $b_i^j$ ,  $c_i^j$ , and  $w_i$  for  $i=1,2$  and  $j=1,\dots,5$ . Therefore, the learning rules can be derived as follows:

$$a_i^j(k+1) = a_i^j(k) - \eta_a \frac{\partial E}{\partial a_i^j} \quad (16)$$

$$b_i^j(k+1) = b_i^j(k) - \eta_b \frac{\partial E}{\partial b_i^j} \quad (17)$$

$$c_i^j(k+1) = c_i^j(k) - \eta_c \frac{\partial E}{\partial c_i^j} \quad (18)$$

$$w_j(k+1) = w_j(k) - \eta_w \frac{\partial E}{\partial w_j} \quad (19)$$

where  $k=0,1,2,\dots$  is the training index,  $\eta$  is the learning rate.

Moreover, the derivatives can be found from Eqs. (14) and (15) and shown as

$$\frac{\partial E}{\partial a_i^j} = \frac{\mu_j(\mathbf{x})}{\sum_{j=1}^s \mu_j(\mathbf{x})} (y - y^d)(w_j - y) \frac{\left[ \left( \frac{x - c_i^j}{a_i^j} \right)^2 \right]^{b_i^j}}{\mu_{A_i^j}^2(x_i)} \frac{2b_i^j}{a_i^j} \quad (20)$$

$$\frac{\partial E}{\partial b_i^j} = \frac{\mu_j(\mathbf{x})}{\sum_{j=1}^s \mu_j(\mathbf{x})} (y - y^d)(w_j - y) \frac{\left[ \left( \frac{x - c_i^j}{a_i^j} \right)^2 \right]^{b_i^j}}{\mu_{A_i^j}^2(x_i)} (-2) \ln \left( \frac{x - c_i^j}{a_i^j} \right) \quad (21)$$

$$\frac{\partial E}{\partial c_i^j} = \frac{\mu_j(\mathbf{x})}{\sum_{j=1}^s \mu_j(\mathbf{x})} (y - y^d)(w_j - y) \frac{\left[ \left( \frac{x - c_i^j}{a_i^j} \right)^2 \right]^{b_i^j}}{\mu_{A_i^j}^2(x_i)} \frac{2b_i^j}{(x - c_i^j)} \quad (22)$$

$$\frac{\partial E}{\partial w_j} = \frac{\mu_j(\mathbf{x})}{\sum_{j=1}^s \mu_j(\mathbf{x})} (y - y^d) \quad (23)$$

Based on these update rules, the training algorithm can be summarized as in the [18].

#### 4.2 Vibration Suppression Controller (VSC)

The controller for suppression vibratory motion can be dominated by piezo-material. The sensors are used to get the information on modal state variables, which are further processed for modal control forces. The actual control inputs are synthesized and applied to the system through piezoelectric actuators.

The voltage across the faces of a distributed piezoelectric sensor subjected to strain due to bending of a beam, is given as [9, 19]

$$V_s(t) = -(Q_0 / C) \int_{l_1}^{l_2} w''(x,t) \eta(x) dx \quad (24)$$

where  $Q_0$  is the charge coefficient which depends on the piezoelectric constant and geometric parameters,  $C$  is the capacitance of the sensor,  $w''(x,t)$  is the beam curvature,  $\eta(x)$  is the spatial distribution of the sensor segment,  $l_1$  and  $l_2$  are the boundary coordinates of the sensor. Moreover,  $\phi_i'(x)$  is the slope of the mode shape function evaluated at  $x$  and  $q_i(t)$  is the modal coordinate corresponding to the  $i$ th mode. Compared to strain gauges, piezoelectric sensors offer superior signal to noise ratio, and better high-frequency noise rejection. Therefore, piezoelectric sensors are quite suitable for applications that involve measuring low strain levels [20]. Therefore, the feedback control law can be chosen the

piezoelectric sensor output voltage  $V_s$  and its rate variables  $\Delta V_s$  as two commonly used variables in the control. The proposed fuzzy vibration suppression controller (VSC) applies the vibration states  $V_s$  and their rate variables  $\Delta V_s$  as inputs, with the voltage applied to the voltage amplifier as the output. Since the vibration suppression controller is independent of linear motion stage positioning control, the individual fuzzy controller is easy to design for each collocated actuator-sensor pair. Moreover, the derivation for the parameter learning for vibration suppression controller is the same as FTC which is shown in Section 4.1. Therefore, the feedback voltage applied across the piezoelectric actuator may be decided by the control algorithm used in Section 4.

#### IV. RESULTS AND DISCUSSIONS

##### (i) Experimental Results of the Moving Cart Subjected to Sinusoidal Trajectory Command

The overall results of the experimental results for the application of the proposed controller for such structure are described in this section. The calculation for controlling results is obtained by the aforementioned procedures shown in section IV. In order to reject the signal noise from the servo motor of the moving cart, the sensor filter is designed as  $1/(s+1)$  for the vibration suppression controller (VSC). To characterize the tracking controller, an ANFIS network with the fuzzifier processing two inputs, the rule base containing 25 rules and the defuzzifier comprising one output was trained. During the training, the network achieved a very good output prediction with a mean square error 0.0024462 after 100 epochs for the tracking controller.

Figure 7 plots the time response for the experimental results of the moving cart for sinusoidal trajectory command under FTC. The tracking response for the moving cart subjected to sinusoidal command is shown in Fig. 7(a). It is seen that a FTC plays well transient performance in the experiment for tracking purpose. In addition, Fig. 7(b) shows the responses for vibrational displacement of the flexible beam with and without PD vibration suppression controller (VSC) under the same FTC. It can be observed that the Fig. 7(b) demonstrates that the performance has been significantly improvement for vibrational displacement while the PD type VSCC applied. Similarly, it can also be demonstrated that the vibrational displacement was clearly reduced once the fuzzy VSCC was introduced (Fig. 7(c)).

To further verify the performance of the proposed controller, Table 1 makes a comparison of the Normalized root mean square (RMS) piezo-sensor output voltage subjected to sinusoidal command for the different control methodologies. From Table 1, it is seen that a FTC plus VSC can reduce the vibrational displacement significantly. This experimental finding proves that the active vibration suppression controller reduces the vibrational displacement owing to uncontrolled vibration by approximately 40% under collocated actuator/sensor pairs, and around 35% for non-collocated pairs. Compared with the system with collocated and noncollocated actuator/sensor pairs, the

performance of the vibration VSCC is considerably better than that of the VSCN in vibration reduction. Moreover, the vibrational displacement can be further reduces to 45% while the fuzzy VSCC applied and 37% vibration reduction once the fuzzy VSCN introduced. Such a controller is observed to result in suppression of the transverse deflection of the structure. It express that the proposed FTC with VSC control scheme can reduce the vibrational displacement effectively, especially in fuzzy VSCC. These experimental results verify the effectiveness of the proposed control methodology for minimizing vibrational displacement in the time domain.

(ii) Experimental Results of the Moving Cart Subjected to Vary Amplitude Sinusoidal Command

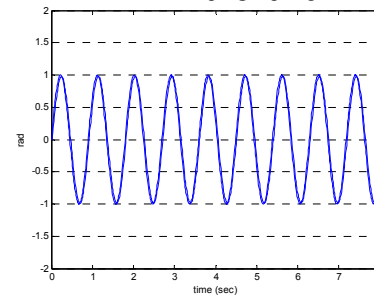
The tracking response for the moving cart subjected to vary amplitude sinusoidal command is shown in Fig. 8(a). It also can see that a FTC plays well transient tracking performance in the experiment for such case. In addition, Fig. 8(b) shows the responses for vibrational displacement of the flexible beam with and without PD vibration suppression controller (VSC) under the same FTC. Moreover, Fig. 8(c) also indicates that the vibrational displacement was clearly reduced while the fuzzy VSCC applied. These experimental results display that the proposed control system achieves excellent tracking performance and satisfactorily attenuates vibration due to flexible beam.

Moreover, Table 2 makes a comparison of the Normalized root mean square (RMS) piezo-sensor output voltage subjected to vary amplitude sinusoidal command for the different control methodologies. Evidently, a vibration reduction (%) for PD VSCC is 44.3% and VSCN is 43.5%. Furthermore, the vibrational displacement can be further reduces to 52.1% while the fuzzy VSCC applied and 50.5% vibration reduction once the fuzzy VSCN introduced. This investigation results also demonstrate that the fuzzy type vibration controller can significantly outperform PD type vibration controller.

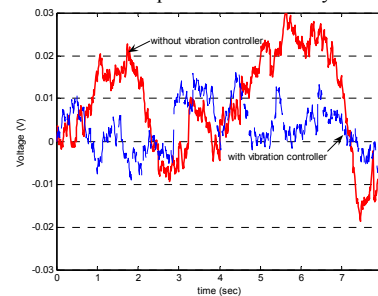
REFERENCES

[1]. H.P. Lee, "Dynamic response of a beam with a moving mass," *Journal of Sound and Vibration*, Vol. 191, No. 2, 1996, pp. 289-294.  
 [2]. U. Lee, "Separation between the flexible structure and the moving mass sliding on it," *Journal of Sound and Vibration*, Vol. 209, No. 5, 1998, pp. 867-877.  
 [3]. S. Park, W.K. Chung, Y. Youm, and J.W. Lee, "Motion analysis of a moving elastic beam with a moving mass," *Proc. of IEEE/ASME International Conference on Advanced Intelligent Mechatronics*, Atlanta, GA, 1999, pp. 167-172.  
 [4]. S. Park, W.K. Chung, Y. Youm, and J.W. Lee, "Natural frequencies and open-loop responses of an elastic beam fixed on a moving cart and carrying an intermediate lumped mass," *Journal of Sound and Vibration*, Vol. 230, No. 3, 2000, pp. 591-615.  
 [5]. S. Park and Y. Youm, "Motion of a moving elastic beam carrying a moving mass-analysis and experimental verification," *Journal of Sound and Vibration*, Vol. 240, No. 1, 2001, pp. 131-157.  
 [6]. S. Park, B.K. Kim, and Y. Youm, "Single-mode vibration suppression for a beam-mass-cart system using input preshaping with a robust internal-loop compensator," *Journal of Sound and Vibration*, Vol. 241, No. 4, 2001, pp. 693-716.

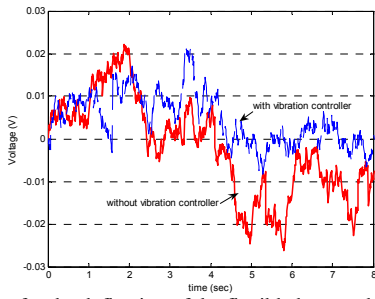
[7]. U.C. Gu and C.C. Cheng, "Vibration analysis of a high-speed spindle under the action of a moving mass," *Journal of Sound and Vibration*, Vol. 278, 2004, pp. 1131-1146.  
 [8]. J. Lin, "Multi-timescale fuzzy controller for a continuum with a moving oscillator," *IEE Proceedings - Control Theory and Applications*, Vol. 151, No. 3, pp. 310-318, 2004.  
 [9]. B. Samanta, "Active control of flexible robot arms using the concept of intelligent structures," *IEEE International Workshop on Intelligent Robots and Systems*, 1990, pp. 941-947.  
 [10]. S. Chen and Z. Cao, "A new method for determining locations of the piezoelectric sensor/actuator for vibration control of intelligent structures," *Journal of Intelligent Material Systems and Structures*, Vol. 11, 2000, pp. 108-115.  
 [11]. D. Halim and S.O.R. Moheimani, "Spatial resonant control of flexible structures-application to a piezoelectric laminated beam," *IEEE Transactions on Control System Technology*, Vol. 9, No. 1, 2001, pp. 37-53.  
 [12]. S.O.R. Moheimani, "Experimental verification of the corrected transfer function of a piezoelectric laminated beam," *IEEE Transactions on Control System Technology*, Vol. 8, No. 4, 2001, pp. 660-666.  
 [13]. A.J. Fleming, S. Behrens, S.O.R. Moheimani, "Optimization and implementation of multimode piezoelectric shunt damping systems," *IEEE/ASME Transactions on Mechatronics*, Vol. 7, No. 1, 2002, pp. 87-94.  
 [14]. G. Wang and N.M. Wereley, "Spectral finite element analysis of sandwich beams with passive constrained layer damping," *Transactions of the ASME, Journal of Vibration and Acoustics*, Vol. 124, 2002, pp. 376-386.  
 [15]. L. Meirovitch, *Computational Methods in Structural Dynamics*, MD: Sijthoff & Noordhoff, 1980.  
 [16]. M.L. James, G.M. Smith, J.C. Wolford, P.W. Whaley, *Vibration of mechanical and structural systems: with microcomputer applications*, 1989.  
 [17]. J. Lin and C.H. Chen, "A novel fuzzy logic approach with friction estimation for positioning and tracking of a linear motion stage system," *ISA Transaction*, Vol. 46/3, pp. 327-342, 2007.  
 [18]. J. Lin and Z.-Z. Huang, "A hierarchical fuzzy approach to supervisory control of robot manipulators with oscillatory bases," *IFAC Mechatronics*, Vol. 17, No. 10, pp. 589-600, 2007.  
 [19]. B. Samanta, "Active Control of Flexible Robot Arms Using the Concept of Intelligent Structures," *IEEE International Workshop on Intelligent Robots and Systems*, pp. 941-947, 1990.  
 [20]. S.O. Reza Moheimani and A.J. Fleming, *Piezoelectric Transducers for Vibration Control and Damping*, Springer 2006.



(a) Response for the cart's position under fuzzy tracking controller

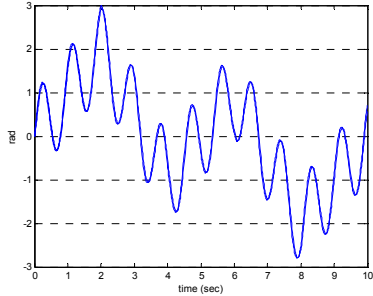


(b) Response for the deflection of the flexible beam subjected to PD vibration suppression controller

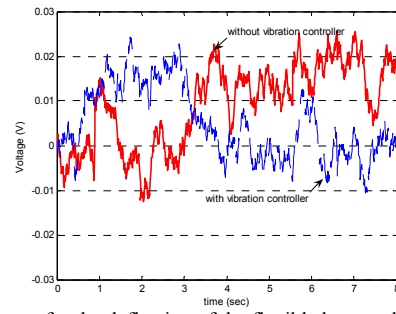


(c) Response for the deflection of the flexible beam subjected to fuzzy vibration suppression controller

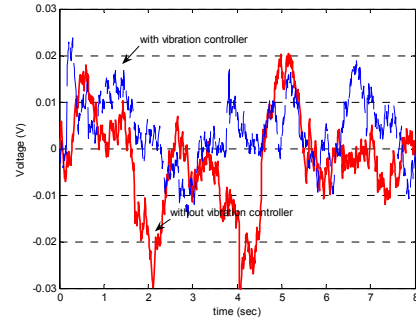
Fig. 7 Experimental Results of the Moving Cart for Sinusoidal Trajectory Command



(a) Response for the cart's position under fuzzy tracking controller



(b) Response for the deflection of the flexible beam subjected to PD vibration suppression controller



(c) Response for the deflection of the flexible beam subjected to fuzzy vibration suppression controller

Fig. 8 Experimental Results of the Moving Cart under Vary Amplitude Sinusoidal Command

Table 4 Normalized RMS vibrational displacement subjected to sinusoidal command

Control Type							
Tracking Controller (PD Type) No Vibration Controller (A)	Tracking Controller (Fuzzy Type) No Vibration Controller (B)	Tracking Controller ( $k_p=7, k_d=0.1$ ) Vibration Controller ( $k_p=0.1, k_d=0.1$ )		Tracking Controller (Fuzzy Type) Vibration Controller ( $k_p=0.1, k_d=0.1$ )		Tracking Controller (Fuzzy Type) Vibration Controller (Fuzzy Type)	
		Collocated actuator-sensor pairs (C)	NonCollocated actuator-sensor pairs (D)	Collocated actuator-sensor pairs (E)	NonCollocated actuator-sensor pairs (F)	Collocated actuator-sensor pairs (G)	NonCollocated actuator-sensor pairs (H)
4.484e-4	4.325e-4	2.653e-4	2.894e-4	2.586e-4	3.029e-4	2.482e-4	2.821e-4
Reduction (%)	(A-B)/A 3.5%	(A-C)/A 40.8%	(A-D)/A 35.4%	(A-E)/A 42.7%	(A-F)/A 32.5%	(A-G)/A 44.6%	(A-H)/A 37.1%
Reduction (%)	(A-B)/A 3.5%	(B-C)/B 38.7%	(B-D)/B 33.1%	(B-E)/B 40.2%	(B-F)/B 30.0%	(B-G)/B 42.6%	(B-H)/B 34.8%

Table 5 Normalized RMS vibrational displacement subjected to vary amplitude sinusoidal command

Control Type							
Tracking Controller (PD Type) No Vibration Controller (A)	Tracking Controller (Fuzzy Type) No Vibration Controller (B)	Tracking Controller ( $k_p=7, k_d=0.1$ ) Vibration Controller ( $k_p=0.1, k_d=0.1$ )		Tracking Controller (Fuzzy Type) Vibration Controller ( $k_p=0.1, k_d=0.1$ )		Tracking Controller (Fuzzy Type) Vibration Controller (Fuzzy Type)	
		Collocated actuator-sensor pairs (C)	NonCollocated actuator-sensor pairs (D)	Collocated actuator-sensor pairs (E)	NonCollocated actuator-sensor pairs (F)	Collocated actuator-sensor pairs (G)	NonCollocated actuator-sensor pairs (H)
4.913e-4	4.636e-4	2.737e-4	2.777e-4	2.508e-4	2.520e-4	2.353e-4	2.432e-4
Reduction (%)	(A-B)/A 5.6%	(A-C)/A 44.3%	(A-D)/A 43.5%	(A-E)/A 48.9%	(A-F)/A 48.7%	(A-G)/A 52.1%	(A-H)/A 50.5%
Reduction (%)	(A-B)/A 3.5%	(B-C)/B 41%	(B-D)/B 40.1%	(B-E)/B 45.9%	(B-F)/B 45.6%	(B-G)/B 49.2%	(B-H)/B 47.5%